



Mostar area land surface temperature determination with satellite methods

Stručni rad/ Professional paper
Primljen/Received: 14. 5. 2018.;
Prihvaćen/Accepted: 14. 6. 2018.

Tea Duplančić Leder

Faculty of Civil Engineering, Architecture, and Geodesy, University of Split, full professor

Nenad Leder

Faculty of Maritime Studies, University of Split, assistant professor

Abstract: The article briefly presents the most critical factors that affect the soil temperature. Most of these factors can be found in city of Mostar area. The simplest and the most widely used method of land surface temperature determination is processing of thermal bands of satellite scenes. Landsat is the longest and most widely used satellite mission with open data. For the purposes of this study Landsat 5, 7 and 8 satellite scenes and open meteorological data were used, from which the atmospheric correction, and then land surface temperature (LST), were calculated for Mostar area. Four winter scenes (taken in the colder part of the year) and four summer scenes (taken in the warmest part of the year) were used. From all processed data, it can be concluded that Mostar can be considered as one of the warmest cities in Bosnia and Herzegovina and wider.

Key words: Land surface temperature, Landsat mission, remote sensing, urban heat islands

Određivanje površinske temperature tla grada Mostara satelitskim metodama

Sažetak: U članku su ukratko prikazani najkritičniji faktori koji utječu na temperaturu tla. Većina se tih čimbenika može naći na području grada Mostara. Najjednostavniji i najčešće korištena metoda određivanja površinske temperature tla je obrada termalnih kanala satelitskih scena. Landsat je najduža i najraširenija satelitska misija s slobodnim podacima. Za potrebe ovog istraživanja su korišteni Landsat 5, 7 i 8 satelitske scene i slobodni meteorološki podaci iz kojih su izračunate atmosferske korekcije, a zatim površinska temperatura tla (PTT) za područje Mostara. Korištene su četiri zimska scene (uzete u hladnijem dijelu godine), i četiri ljetne scene (uzete u najtoplijem dijelu godine). Iz obrađenih se podataka može zaključiti da se Mostar može smatrati jednim od najtoplijih gradova u Bosni i Hercegovini i šire.

Ključne riječi: površinska temperatura tla, Landsat misije, daljinska detekcija, urbani toplinski otoci

1. INTRODUCTION

Today, 54% of the global population lives in urban areas, and by the middle of the century it is expected that this percentage will be 66%, and the total area of urban land will significantly increase. The growing urbanization causes changes in temperature balance in densely developed urban areas due to anthropogenic effects. Surface air and soil temperatures are an important factor in urban climatology studies [1, 2, 3]. Thermal remote sensing is used in urban areas to observe the effects of urban heat islands (UHIs), to determine and classify land cover and as input data for surface atmosphere change models over urban areas [3, 4, 5].

UHIs are parts of urban areas where air and soil temperatures are higher than in the surrounding area (Figure 1). They develop as a result of the fact that predominant urban materials, such as concrete, asphalt or brick, heat up differently than natural materials such as soil, water or vegetation, and can increase the temperature of urban areas by several degrees in relation to rural areas [6]. In the summer period, the air temperature is at its maximum usually about 4 p.m. [6, 7]. In the summer, the highest temperature differences are observed in the cities located in lowland areas or valleys and having over 100,000 inhabitants [8]. In these places, the temperature differences can be 12°C and more [6, 7].

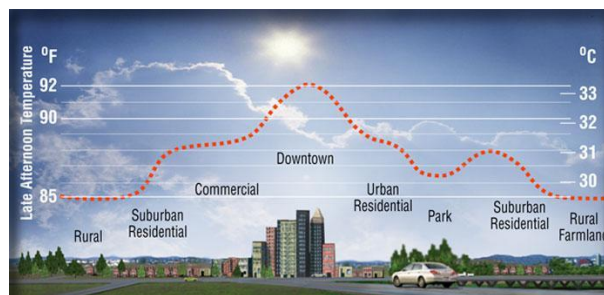


Figure 1 Urban heat islands; [8]

The effects of urban heat islands are greater and locally have more distressing and significant consequences than the greenhouse effect. UHIs are generally caused by [9]:

- Loss of natural vegetation and its replacement with vapor proof materials that cause reduced evapotranspiration, reduced humidity and dryness of urban areas;
- Anthropogenic impacts (exhaust gases, industry, refrigerating devices) [10, 11].
- Dominant urban building materials with high thermal energy emissions and high thermal inertia [12, 13];
- Parts of urban geometry, e.g. urban canyons, particularly in city centers, which increase heating of surfaces and thermal energy absorption, and block the circulation of air masses that cool the space;
- Albedo or solar energy reflection coefficient is different for different materials, and is shown in Table 1 [12, 13].

On the other hand, UHIs do not occur in rural areas due to high evapotranspiration and large areas of shade created by vegetation and water areas.

Reported in large numbers in recent years, heat strokes are becoming increasingly frequent and more significantly affect the quality of life and human health (cardiovascular, allergic and contagious diseases). Vulnerable groups are the poorer and older populations with limited ability to adapt, and the population dependent on outdoor work.

The aim of the paper is, using remote sensing methods, to investigate the microclimate changes in land surface temperature in the Mostar city area, presence of UHIs and their



potential temporal and seasonal variability. The results of the research should identify the affected and critical heat areas to the persons responsible for planning and inform them about the measures for reduction of surface air and soil temperatures.

1. STUDY AREA

Bosnia and Herzegovina (B&H) is situated in southeastern Europe, and Herzegovina-Neretva Canton is located in the southern part of the country, occupies 4,401 km² or 16.9% of its area [14], and is the second largest canton in B&H. The canton mainly extends along the Neretva River valley and includes the parts of Herzegovina west of the city of Mostar, the administrative center of the canton (Figure 2).

Bosnia and Herzegovina is a mountainous area and belongs to the western part of the Mediterranean Zone. Herzegovina has a hilly and mountainous relief with numerous depressions and basins [15, 16] (Figure 2).



Figure 2 Elevation map of the wider area of the city of Mostar (left) Location of the administrative area of the city of Mostar (right)

Mostar is the administrative center of the southern part of B&H with a total population of 113,169 [14] and represents the most important city of the Herzegovina region, as well as the cultural center and center of Herzegovina-Neretva Canton. The settlement on the Neretva River, between the Čabulja and Velež mountains, has existed since prehistoric times (Figure 2).

2.1 The climate of the city of Mostar

The climate characteristics of Mostar are considerably influenced by the proximity of the Adriatic Sea, with which it is connected by the canyon of the Neretva River. In the summer months, the occurrence of temperatures over 40°C is not uncommon. The coldest month is January with an average temperature of 5°C, and the warmest month is July with an average temperature of 26°C. Mostar has a relatively dry season from June to September, and the rest of the year is humid with mild climate [16]. The subtype of Köppen climate classification for this climate is Cfa, which means "oceanic climate with hot summers and Mediterranean tendency" (close to Csa climate subtype) [17]. Mostar is the sunniest city in the country with an average of 2291 sunny hours a year [18]. The highest temperature in Mostar was measured on 31 July 1901 and it was 46.2°C [18], which classified the city as the hottest city of the former Yugoslavia, today BiH. It can be generally concluded that the city had a dry climate that is increasingly humid today, which makes the summer heat hardly bearable for people [16].



3 Materials and methods

3.1 Thermal remote sensing

The platforms most commonly used for determining land surface heat are satellites (GEOS, AVHRR, MODIS, LANDSAT, ASTER) with wide spatial coverage [19] and limited time intervals; aircraft with high spatial resolution but high data cost, and ground-based sensors with good temporal resolution and no need for corrections due to atmospheric influences [20];

The first observation of surface thermal islands (with satellite sensors) was published in 1972 [21] and since then, different satellite sensors have been used to detect temperatures of urban areas. Today, authors most commonly use Landsat thermal data to calculate surface temperature since they have a good spatial resolution and are available for use free of charge. All other satellite missions have better temporal but poorer spatial resolution, so their use is less appropriate to realize the main objective of this paper.

The Landsat satellite mission is positioned above the study area every eight days at 9:42 (UTC). The period of day with maximum surface temperature is from 2 p.m. to 6 p.m. [7, 17]. Landsat 5, 7 and 8 satellite images were used in the paper [28]. The satellites used to observe parts of the Earth's surface directly measure radiation of the top of the atmosphere (TOA) [4]. The procedure for calculating land surface temperature is described in Chapter 4.

3.2 Meteorological data

The temperature, air pressure and relative humidity data used for the purposes of this paper were measured at the meteorological station Mostar airport ($\varphi=43,283^{\circ}\text{N}$; $\lambda=17,846^{\circ}\text{E}$; $h=125\text{m}$) for selected meteorological situations (Table 2). These data were used to determine atmospheric correction parameters of the selected Landsat 5, 7 and 8 scenes. According to air temperature measurements, it was shown that the summers 2015-2017 were the warmest summers since the measurements began. These extreme temperature values are expected to continue [22].

3.3 Selection of appropriate Landsat satellite images

Standard Landsat products are distributed by the US Geological Survey's Earth Resources Observation and Science Center (USGS EROS) (<http://earthexplorer.usgs.gov/>), and they include roughly processed and calibrated (geocoded) multispectral images. For the purposes of this study, Landsat 7 and 8 scenes were selected so as to represent one characteristic winter and summer meteorological episode at the beginning of the new millennium and the last three years, which the World Meteorological Organization [22] declared the hottest years in the history of meteorological measurements.

All the Landsat scene pre-processing and processing procedures were conducted in the ArcGIS 10.6 computer program. The final processing of the resulting raster maps and data was conducted using the Adobe Photoshop CS6 program.

3.4 Atmospheric correction

Processing of the satellite images was preceded by pre-processing, which involves elimination of atmospheric scattering from the image. In order to calculate atmospheric correction parameters, atmospheric transmissions and upwelling and downwelling radiances should be known or modeled for a particular area.

The method for determining atmospheric parameters based on the given temperature, pressure and air humidity is used in the paper. The atmospheric correction for the location of Mostar city, and selected date and time, was calculated by the model that uses global atmospheric profiles, modeled in the National Centers for Environmental Prediction (NCEP) [23]. The atmospheric



correction parameter was roughly determined using this method. After modeling the global atmospheric profiles, as well as surface temperatures, with the knowledge of pressure and relative humidity, it is possible to convert the space-reaching radiance to a surface-leaving radiance:

$$L_{TOA} = \tau \varepsilon L_T + L_u(1 - \varepsilon)L_d \quad (1)$$

τ is the atmospheric transmission,

ε is the emissivity of the surface,

L_T is the radiance of a blackbody of kinetic temperature T ,

L_u is the upwelling or atmospheric path radiance,

L_d is the downwelling or sky radiance,

L_{TOA} is the space-reaching or TOA radiance measured by the instrument. The radiances are expressed in $W/m^2 \cdot \text{ster} \cdot \mu\text{m}$, and the transmission and emissivity are unitless.

Radiance was converted to temperature using the Planck equation. The details of atmospheric correction calculations are shown in [24, 25]. Ignoring the atmospheric correction can result in systematic errors in predicting land surface temperature. It should be noted that surface temperature calculated without using the NCEP atmospheric profile models to calculate atmospheric correction is lower by 5-10 °C.

The surface meteorological parameters of the meteorological station in Mostar, as well as atmospheric correction parameters (atmospheric transmission and upwelling and downwelling radiances) for the selected dates and time are shown in Table 1. Table 1 shows the air temperatures measured at the meteorological station Mostar airport. High air and soil temperatures, especially those above 36°C, have a negative effect on human health, because at such temperatures the body is prevented from cooling.

Table 1 Specified meteorological parameters and calculated atmospheric correction for Mostar area (43.82°N, 18.33°E, elevation 511m) for selected dates at 9:42 UTC

| Mostar date | Meteorological parameters | | | Atmospheric correction | | |
|-------------|---------------------------|--------------|---------------|--------------------------|--------------------|----------------------|
| | Air temp.(°C) | Humidity (%) | Pressure (mb) | Atmospheric transmission | Upwelling radiance | Downwelling radiance |
| 02.08.2017. | 31.0 | 40 | 1016 | 0.70 | 2.59 | 4.16 |
| 25.01.2018 | 05.0 | 65 | 1029 | 0.94 | 0.35 | 0.60 |
| 13.08.2015. | 30.1 | 43 | 1012 | 0.69 | 2.57 | 4.14 |
| 03.12.2015. | 05.0 | 71 | 1031 | 0.94 | 0.39 | 0.67 |
| 18.08.2011. | 28.8 | 42 | 1015 | 0.76 | 1.95 | 3.15 |
| 05.12.2010. | 08.0 | 57 | 1020 | 0.94 | 0.35 | 0.61 |
| 09.08.1999. | 30.1 | 43 | 1012 | 0.73 | 2.17 | 3.51 |
| 16.01.2000. | 03.0 | 40 | 1023 | 0.93 | 0.36 | 0.62 |

3.5 Conversion of digital numbers to temperature

3.5.1. Conversion of a digital number to TOA radiance

The OLI and TIRS band data can be converted to TOA spectral radiance using the radiance rescaling factors provided in the metadata file [26, 27]:

$$L_\lambda = M_L Q_{cal} + A_L \quad (2)$$

L_λ is the TOA spectral radiance (Watts/(m²*srad*μm));

M_L is the band-specific multiplicative rescaling factor from the metadata file;

A_L is the band-specific additive rescaling factor from the metadata file;

Q_{cal} is the quantized and calibrated standard value of a graphical element (digital number DN).



3.5.2 Conversion of radiance to TOA reflectance

OLI band data can also be converted to TOA planetary reflectance using reflectance rescaling coefficients provided in the product metadata file (MTL file). The following equation is used to convert DN values to TOA reflectance for OLI data:

$$\rho_{\lambda}' = M_{\rho} Q_{cal} + A_{\rho} \quad (3)$$

ρ_{λ}' is the TOA planetary reflectance, without correction for solar angle;

M_{ρ} is the band-specific multiplicative rescaling factor from the metadata file;

A_{ρ} is the band-specific additive rescaling factor from the metadata file;

Q_{cal} is the roughly pre-processed and calibrated standard value of a graphical element (digital number DN).

3.5.3 TOA reflectance with correction for solar angle

The TOA reflectance with correction for solar angle is:

$$\rho_{\lambda} = \frac{\rho_{\lambda}'}{\cos(\theta_{SZ})} = \frac{\rho_{\lambda}'}{\cos(\theta_{SE})} \quad (4)$$

ρ_{λ} is the TOA planetary reflectance;

θ_{SE} is the local sun elevation angle. The scene center sun elevation angle in degrees is provided in the metadata file;

θ_{SZ} is the local solar zenith angle;

$$\theta_{SZ} = 90^{\circ} - \theta_{SE}.$$

For more accurate reflectance calculations, per pixel solar angles should be known instead of the scene center solar angle. The solar zenith angle of scene center pixel can be obtained in the Landsat image metadata file.

3.5.4 Conversion to at-satellite brightness temperature

Temperature radiance conversion can be performed using the Planck equation [28]. TIRS band data can be converted from spectral radiance to brightness temperature using the thermal constants provided in the metadata file:

$$T = \frac{K_2}{\ln\left(\frac{K_1}{L_{\lambda}} + 1\right)} \quad (5)$$

T is the at-satellite brightness temperature (K);

L_{λ} is the TOA spectral radiance (Watts/(m²*srad*μm)),

K_1 and K_2 are band-specific thermal conversion constants and they are $K_1=666.09$ and $K_2=1282.71$ for Landsat 7 data, while for Landsat 8 band 10 they are $K_1=774.88$ and $K_2=1321.08$.

Temperature ranges were shown using unsupervised classification, which proved to be more readable for different temperature ranges in winter and in summer.

4 Results

Four summer and four winter scenes, recorded at intervals of 5 to 10 years, were compared. The interval of the last two scenes is two years and they represent the beginning of more visible



climate changes. The scenes were selected so as to represent the coldest (December and January) and the warmest (August) parts of the year in the observed area. Unfortunately, the observed scenes were not equally distributed in time intervals due to freely available meteorological information, poor availability of older scenes, and errors on Landsat 7 sensors, which reduced the quality of data (this is particularly related to heat data that are highly unstable for interpolation and unsafe for use).

However, when comparing these scenes, significant differences are evident in the quantity of vegetation and temperature ranges in the observed area. Figure 3 shows the normalized differential vegetation index (NDVI) for the selected summer scenes. The figure shows that NDVI is low in the wider Mostar city area (southern part of the area) and in the Prenj mountain area (northeastern part of the area), indicating the condition of vegetation. This fact has a significant effect on reflection in the thermal part of the spectrum (Figure 4), so that high land surface temperatures can be read in the urban area. In the mountain area, high temperatures are not evident due to the high altitudes of the area, decrease of temperature with altitude, and the possibility of fog, dew and low clouds in lower layers.

Figure 4 shows the summer land surface temperatures (LSTs) obtained from reflection in thermal band 10, calibrated for the atmospheric correction calculated according to meteorological data (Table 3). On the right side of Figure 4 (13 Aug 2015) the maximum temperature range (0.7-54.5°C) can be observed, as a result of climate changes in recent years. Landsat satellite passes over this area several minutes before 10 a.m., and the temperature maximum can be expected from 12 Noon to 4 p.m.. This would mean that at least 2 to 3°C should be added to determined temperatures in order to obtain the maximum daily land temperature, which in the case of 2017 means even up to 60°C.

At the end of the millennium in the summer part of the year (9 Aug 1999), temperatures ranged from 8.7 to 35.7°C. On 18 Aug 2011, Prenj mountain was most probably under fog or low clouds because the measured temperature was -1.9°C at about 10 a.m., while the temperature in the urban area reached 48°C. The large temperature difference can also be attributed to the big difference in height between the calibration point (altitude 50m) and the temperature determination point (Figure 4). In 2015, which was declared as one of the three hottest years since the measurements began, the lowest determined temperature was 0.7°C, while the maximum temperature reached 54.5°C. An even higher temperature maximum was recorded on 2 Aug 2017, when the lowest temperature was 19.9°C, while the highest recorded temperature was an impressive 59.6°C (Figure 4).

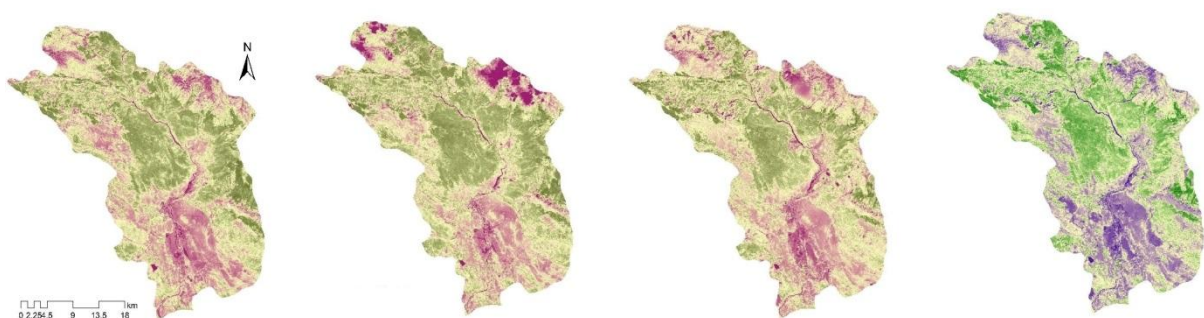


Figure 3 NDVI of summer scenes 9 Aug 1999 (left), 18 Aug 2011 (center left), 13 Aug 2015 (center right), and 2 Aug 2017 (right), of the Mostar city area

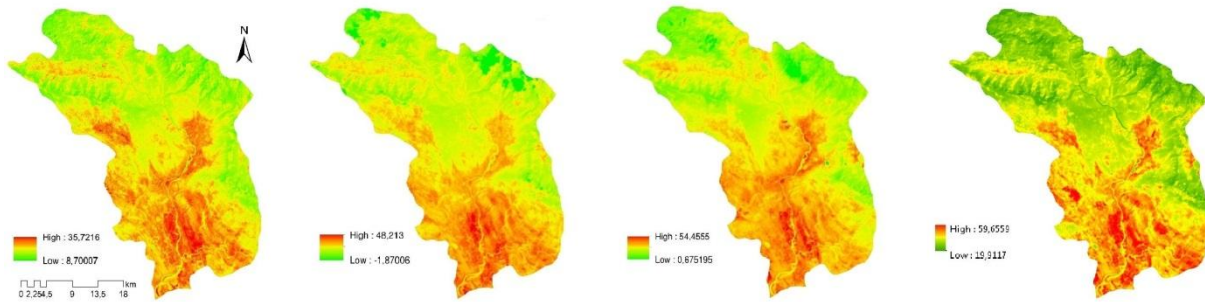


Figure 4 LST of summer scenes 9 Aug 1999 (left), 18 Aug 2011 (center left), 13 Aug 2015 (center right) and 2 Aug 2017 (right), of the Mostar city area

NDVI of winter scenes are significantly different from those of summer scenes. In scenes taken on 16 Jan 2000 and 5 Dec 2010, we can observe a low vegetation index in the southwestern part of the area, which is the flooded area of Mostarsko Blato. On the other hand, on the Čabulja mountain in the northwestern area of the scene from 2000, there is an area that was later covered with vegetation, and it can be concluded that this area was scorched by fire or otherwise lost vegetation cover (for example, covered with snow) (Figure 5).

It can also be seen that the temperature ranges are significantly differently distributed in the winter season than in the summer season (Figures 4 and 6). At the beginning of the millennium in 2000, the minimum temperature was -5.9°C and the maximum temperature reached 13.0°C . Ten years later, also in the coldest period of the year, the minimum recorded temperature was -15.0°C and the maximum one was 13.1°C . The largest temperature range was recorded on 3 Dec 2015, and it was a minimum of -21.1°C (the value applies to the lowest temperature of land unmasked by clouds in the northwestern part of the study area, extending across the area of Čabulja and Čvrstica mountains), while the maximum was 20.1°C (Figure 6).

The highest land temperature in the summer period was expectedly recorded in the urbanized city basin area in Mostar, while the lowest temperature was recorded on top of the Prenj mountain.

Finally, it can be emphasized that the course of the Neretva River can be identified in all the presented NDVI and LST scenes. In the winter part of the year the river is warmer and in the summer colder than the environment.

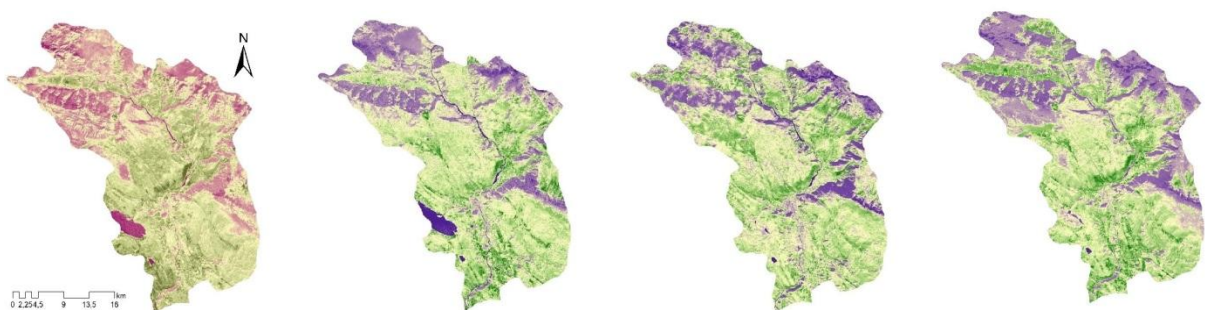


Figure 5 NDVI of winter scenes 16 Jan 2000 (left), 5 Dec 2010 (center left) and 3 Dec 2015 (center right) and 25 Jan 2018 (right) of the Mostar city area

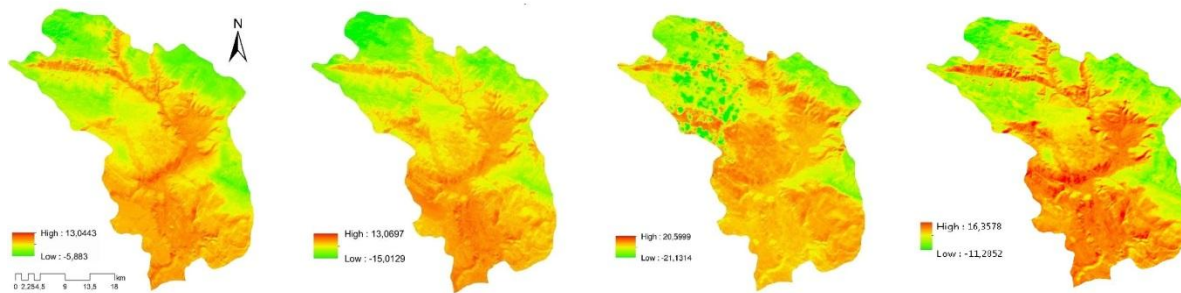


Figure 6 LST of winter scenes 16 Jan 2000 (left), 5 Dec 2010 (center left) and 3 Dec 2015 (center right) and 25 Jan 2018 (right) of the Mostar city area

5 Discussion

The paper attempted to investigate the microclimate changes in land surface temperature and presence of UHIs and their temporal and seasonal variability in the Mostar city area. A significant increase in land surface temperature is visible from a number of thermal satellite images. Maximum temperatures occur from 2 p.m. to 4 p.m., so the presented temperatures should be additionally increased by several degrees and they can reach over 60°C.

In the last ten years or so, there have been a large number of scientific papers and studies looking into climate changes, which result in the development of disaster maps and preparation of documents for studies of risks and environmental protection from heat disasters.

Studies of thermal characteristics of urban areas and reduction of heat island effects [7] are mainly based on denser urban vegetation, use of reflective roofing materials with special emphasis on green roofs, and use of cool reflective pavements. Increasing vegetation and water surfaces lead to a decrease of LSTs and UHIs, and therefore municipal utility companies are advised to increase such areas.

In this region, different authors have recently begun to deal with microclimate characteristics of certain cities, and thereby with advancement in climate characteristics and improvement in the quality of life in a particular area [7, 29, 30].

6 Conclusion

The method of using satellite sensors with thermal bands for determining land surface temperatures is often used for scientific research as well as for land planning and management. This paper has established that Mostar, the city where maximum temperatures were measured, is also the city where maximum temperature of soil can be expected too. The city of Mostar is probably the hottest city in BiH and beyond since it is located in a valley or canyon in the sub-Mediterranean region, which increasingly accumulates heat energy. Outside the city of Mostar, a significant part of the mountainous terrain is steeply sloped with a small amount of vegetation, which also increases the emission of infrared radiation.

Finally, it can be concluded that this study can help urban and spatial planners in the process of spatial planning to ensure that the heat effect is reduced by using appropriate "green" construction materials and by afforesting urban and rural areas.

REFERENCES

1. Aniello, C.: *Mapping Micro-urban Heat Islands Using LANDSAT TM and a GIS*, Computers & Geosciences, 21 (1995) 8, pp. 965-967.



2. Emery J.; Oke T.; Roth, M.: *Satellite-Derived Urban Heat Islands from Three Coastal Cities and the Utilization of Such Data in Urban Climatology*, International Journal of Remote Sensing (1989) 10, pp. 1699-1720.
3. Oke, T.R.: *Boundary layer climates*, 2nd. Methuen, 1987.
4. Voogt, J.A., Oke, T.R.: *Thermal remote sensing of urban climates*, Remote Sensing Environmental (2003) 86, pp. 370–384.
5. Jimenez-Munoz, J.C.; Sobrino, J.: *A generalized single-channel method for retrieving land surface temperature from remote sensing data*, Journal of Geophysical Research, 108 (2004) 22, pp. 4688.
6. Oke, T.R.: *Initial Guidance to Obtain Representative Meteorological Observations at Urban Sites*. World Meteorological Organization, Instruments and Observing Methods, IOM Report No. 81, WMO/TD-No. 1250, 2006.
7. Babić, S., Deluka-Tibljaš, A., Cuculić, M., Šurdonja, S.: *Analysis of pavement surface heating in urban areas*, Građevinar 64 (2012) 2, pp. 127-134.
8. Berkeley Lab, Heat island group, <https://heatland.lbl.gov>. (10.06.2016.).
9. Voogt, J. A.: *Urban Heat Island (Chapter)*, Encyclopedia of Global Environmental Change (Munn, T., ed.), 3, 660-666 Chichester, Wiley, 2002.
10. De Munck, C.; Pigeon, G.; Masson, V.; Meunier, F.; Bousquet, P.; Tremeac, B.; Merchat, M.; Poef, P.; Marchadier, C.: *How much can air conditioning increase air temperatures for a city like Paris, France?*, International Journal of Climatology, 33 (2013) 1, pp. 210 – 227.
11. Oke, T.R.: *Urban Environments - The Surface Climates of Canada*, McGill-Queen's University Press, Montreal, 1997.
12. Environmental Fluid Dynamics - LUMPS Project, <http://mech.utah.edu/~pardyjak>. (10.06.2016.).
13. The URBANFLUXES idea, <http://urbanfluxes.eu>. (10.06.2016.).
14. Šiljković, Ž.; Čuljak, M.: *Transformation of Rural Settlements of the City of Mostar in the Second Half of the Twentieth Century*, Geoadria 20/1 (2015) 41-52.
15. Radusin, S; Oprašić, S.; Cero; M. Abdurahmanović, I.; Vukmir, G.: *Drugi nacionalni izvještaj Bosne i Hercegovine u skladu s okvirnom konvencijom ujedinjenih nacija*, 2003.
16. "Bosnia and Herzegovina" in Geo-Data: The World Geographical Encyclopedia, Gale, 2003.
17. Climate Summary for Mostar, Meteorological Institute of Bosnia and Herzegovina, Sarajevo, 2015.
18. Federalni zavod za statistiku <http://www.fzs.ba>
19. Tomlinson, J.C., Chapman, L., Thornes, J.E., Baker, C: Remote sensing land surface temperature for meteorology and climatology: a review, Meteorological Applications, 18 (2011) 3, pp.
20. Rao, P. K.: Remote sensing of urban heat islands from an environmental satellite, Bulletin of the American Meteorological Society, (1972) 53, 647– 648.
21. Tomlinson, J.C., Chapman, L., Thornes, J.E., Baker, C: Remote sensing land surface temperature for meteorology and climatology: a review, Meteorological Applications, 18 (2011) 3, pp. 296–306.
22. Praćenje i ocjena klime u 2015. godini - Climate monitoring and Assessment for 2015, Državni hidrometeorološki zavod (Pandžić, K., Lisko, T. ed.), Zagreb, 2016.
23. Barsi, J.A.; Schott, J.R.; Palluconi, F.D.; Hook, S.J.: Validation of a Web-Based Atmospheric Correction Tool for Single Thermal Band Instruments, Earth Observing Systems X, ed. Butler, J.J.; Proceedings of SPIE Vol. 5882. 2005. <http://atmcorr.gsfc.nasa.gov>. (10.06.2016.).
24. Schott, J.R.; Brown, S.D.; Barsi, J.A.: Calibration of Thermal Infrared (TIR) Sensors, In J. Luvall & D. Quattrochi (Eds.). Thermal Remote Sensing in Land Surface Processes. United Kingdom, Taylor & Francis. 2004.



25. Barsi, J.A.; Schott, J.R.; Palluconi, F.D.; Helder, D.L.; Hook, S.J.; Markham, B.L.; Chander, G.; O'Donnell, E.M.: Landsat TM and ETM+ Thermal Band Calibration, *Canadian Journal of Remote Sensing*, 28 (2003) 2, pp. 141-153.
26. USGS: *Landsat 8 (L8) Data Users Handbook*, Department of the Interior U.S. Geological Survey, EROS, Sioux Falls, South Dakota, (2015) <http://landsat.usgs.gov>. (10.06.2016.).
27. Lin, B.: *Earth Radiation Budget*, Top of Atmosphere Radiation in *Encyclopedia of remote sensing* (E.G. Njoku ed.), Springer. 2014. pp 145-146.
28. Uysal, M.; Polat, N.: *An investigation of the relationship between land surface temperatures and biophysical indices retrieved from Landsat TM in Afyonkarahisar (Turkey)*, *Technical Gazette* 22, 1(2015), 177-181.
29. Duplančić Leder, T., Leder, N., Hećimović, Ž.: *Split Metropolitan area surface temperature assessment with remote sensing method*, *GRAĐEVINAR*, 68 (2016) 11, pp. 895-905, doi: <https://doi.org/10.14256/JCE.1661>.
30. Duplančić Leder, T., Leder, N.: *Land Surface Temperature Determination in the Town of Mostar Area*, *Technical Gazette* 25, (2018), prihvaćen za tisak - accepted for publishing.